Biochemical and Biophysical Research Communications 447 (2014) 7–11

Contents lists available at ScienceDirect

Biochemical and Biophysical Research Communications

journal homepage: www.elsevier.com/locate/ybbrc

The crystal structure of MPK38 in complex with OTSSP167, an orally administrative MELK selective inhibitor

Yong-Soon Cho [1], YingJin Kang [1], Kuglae Kim, Young-je Cha, Hyun-Soo Cho *

Department of Systems Biology, College of Life Science and Biotechnology, Yonsei University, Seoul 120-749, Republic of Korea

ARTICLE INFO

Article history:
Received 4 March 2014
Available online 18 March 2014

Keywords:
MPK38
MELK
OTSSP167
Inhibitors

ABSTRACT

Murine protein serine/threonine kinase 38 (MPK38), also known as maternal embryonic leucine zipper kinase (MELK), has been associated with various human cancers and plays an important role in the formation of cancer stem cells. OTSSP167, a MELK selective inhibitor, exhibits a strong *in vitro* activity, conferring an IC_{50} of 0.41 nM and *in vivo* effect on various human cancer xenograft models. Here, we report the crystal structure of MPK38 (T167E), an active mutant, in complex with OTSSP167 and describe its detailed protein-inhibitor interactions. Comparison with the previous determined structure of MELK bound to the nanomolar inhibitors shows that OTSSP167 effectively fits into the active site, thus offering an opportunity for structure-based development and optimization of MELK inhibitors.

1. Introduction

Murine protein serine/threonine kinase 38 (MPK38), also known as maternal embryonic leucine zipper kinase (MELK), was initially identified as a murine orthologue of human HPK38/hMELK/KIAA175 [1]. MELK participates in a wide range of cellular processes that are related to the cell cycle [2], apoptosis [3,4], spliceosome assembly [5], and cell proliferation [6]. More importantly, its overexpression has been reported in various human cancers [7–10] and is associated with more aggressive forms of astrocytoma, glioblastoma, breast cancer, and melanoma [11–13]. MELK plays a critical role in the formation or maintenance of cancer stem cells [7,14–16].

Protein kinases are key regulators in signal transduction and in the coordination of complex functions. These play critical roles in growth signaling pathways in cancer cells [17,18]. Its ATP binding pocket has been recognized as an ideal target for pharmacological therapy, and differences in the residues lining its ATP-binding cavity confer selectivity of kinase inhibitors against a specific kinase target [19,20]. For these reasons, protein kinases are considered as attractive therapeutic targets of anti-cancer drugs.

A recent report has shown that the MELK selective inhibitor, OTSSP167, effectively suppresses MELK kinase activity, with an IC_{50} of 0.41 nM and the phosphorylation of MELK substrates such as PSMA1 (proteasome subunit alpha type 1) and DBNL (drebrin-like) [21]. The compound inhibited mammosphere formation in breast cancer cells, which is one of the characteristics of breast cancer stem cells [21]. In addition to its *in vitro* effect, it also exhibited strong growth suppressive effects on various types of human cancer xenografts of breast, pancreas, prostate, and lung cancers, indicating a potential as a novel treatment for a wide range of human cancers [21].

In this study, we present the complex structure of MPK38 (T167E)-OTSSP167 for the purpose of understanding the binding mode of the MELK selective inhibitor and to provide a foundation for structure-guided drug design.

2. Materials and methods

2.1. Protein expression and purification

Residues 1–326 of MPK38 were subcloned into a pET21(b) vector (Novagen). The MPK38 (T167E) mutant was generated using the QuickChange kit (Stratagene). The MPK38 (T167E) construct was transformed into *Escherichia coli* BL21(DE3) cells; MPK38 (T167E) protein was induced by incubating the cells in 0.5 mM IPTG at 18 °C for 16 h. The cells were harvested and suspended in a cell lysis buffer [20 mM Tris–HCl (pH 7.5) and 500 mM NaCl]. Cells were lysed by sonication, and the supernatant was separated by a centrifugation. The cell supernatant was applied to a Histrap HP column (GE Healthcare) and washed with a buffer [20 mM Tris–HCl (pH 7.5), 500 mM NaCl, and 50 mM imidazole]. MPK38 (T167E) was eluted with an elution buffer [20 mM Tris–HCl (pH 7.5), 500 mM NaCl, and 200 mM imidazole]. MPK38 (T167E) was

* Corresponding author.
E-mail address: hscho8@yonsei.ac.kr (H.-S. Cho).
[1] These authors contributed equally to this work.

http://dx.doi.org/10.1016/j.bbrc.2014.03.034
0006-291X/

Table 1
X-ray data collection and refinement statistics.

Data collection	
Space group	$P2_12_12_1$
Unit-cell parameters (Å, °)	a = 35.96, b = 75.76, c = 128.12, $\alpha = \beta = \gamma$ = 90
Resolution (Å)	50–2.57
R_{merge}	0.148 (0.718)
Completeness (%)	100 (100)
Multiplicity	8.2 (8.6)
Refinement	
Resolution (Å)	32.61–2.57
No. of reflections	11,707
R_{work}/R_{free}	0.204/0.251
No. of atoms	
Protein	2,612
Water	34
B factors(Å^2)	
Protein	44.225
Water	37.354
R.m.s. deviations	
Bond lengths(Å)	0.014
Bond angles (°)	1.727

Values in parentheses are for the highest resolution shell.

purified in an anion-exchange column Hitrap Q (GE Healthcare). Finally, MPK38 (T167E) was eluted by gel-filtration chromatography (Hiload 16/60 200 pg, GE Healthcare) with a size-exclusion chromatography (SEC) buffer [20 mM Tris–HCl (pH 7.5), 300 mM NaCl, and 5 mM DTT].

2.2. Crystallization, data collection, and structure determination

The inhibitor OTSSP167, [1-(6-(3,5-dichloro-4-hydroxyphenyl)-4-((*trans*-4-((dimethylamino)methyl)cyclohexyl)amino)-1,5-naphthyridin-3-yl)ethanone] was purchased from Chem Scene. MPK38 (T167E) was concentrated to 15 mg/mL for crystallization screening using a commercial screening kit (Hampton Research). MPK38 (T167E) was mixed with 1 mM of OTSSP167, and a complex crystal was grown at 293 K by a vapor-diffusion method under 0.2 M lithium sulfate, 0.1 M sodium citrate (pH 5.5) and 15% ethanol for 2 weeks. The complex crystal was soaked in a crystallization buffer with 20% ethylene glycol. X-ray diffraction data of the crystals were collected on the BL-17A beamline at the Photon Factory (Japan). The MPK38 (T167E) crystal belongs to the spacegroup $P2_12_12_1$ with a = 35.960 Å; b = 75.760 Å; and c = 128.120 Å in a cell unit. The initial phase of MPK38 (T167E) was obtained by

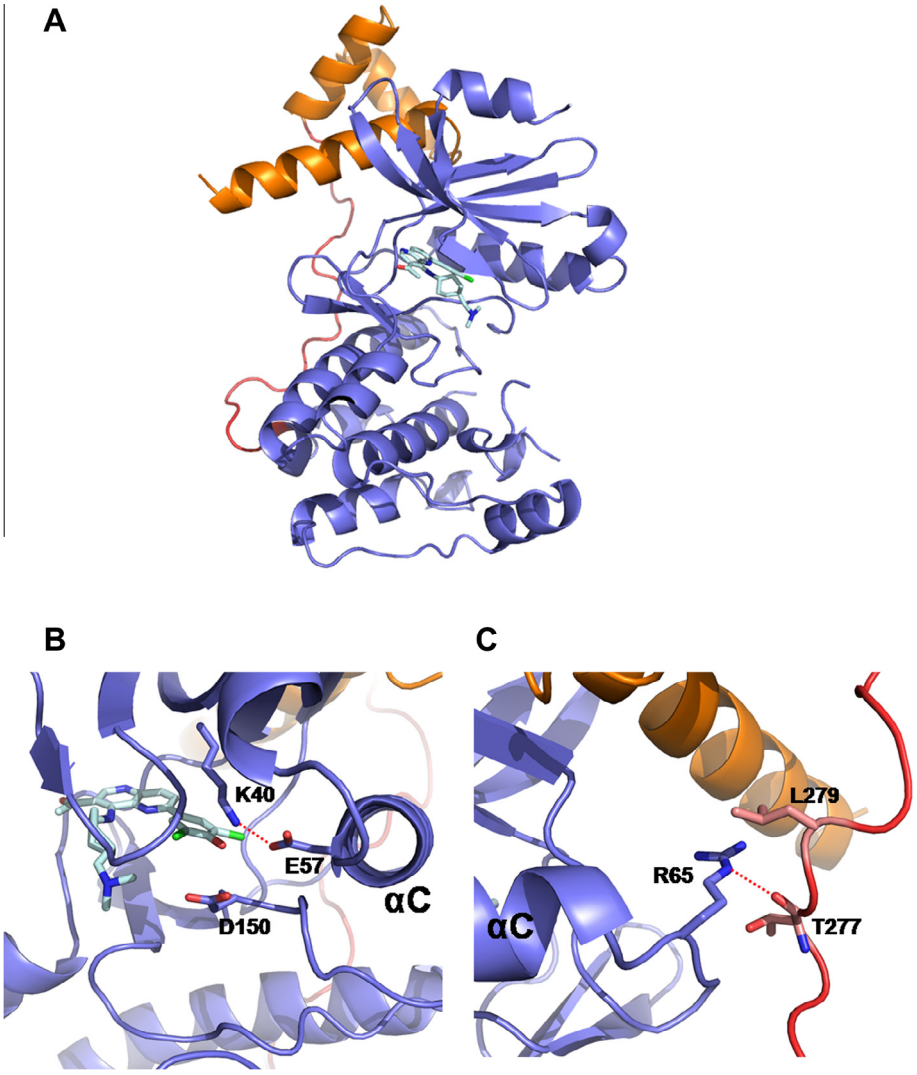

Fig. 1. Crystal structure of MPK38 (T167E)-OTSSP167. (A) Cartoon presentation of the structure of MPK38 (T167E) (kinase domain: blue; UBA linker: red; UBA domain: orange) in complex with OTSSP167. OTSSP167 (cyan) is shown as a stick model. (B) Close-up view of the αC-in and DFG-in conformation. The ionic pair between Lys40 and Glu57 is depicted as a red dashed line. (C) The hydrophobic interaction between Arg65 from αC and Thr277 and Leu279 from the UBA linker is shown. The hydrogen bond between Arg65 and the carbonyl group of Thr277 is displayed as a red dashed line.

molecular replacement (MR) using Molrep [22] using MPK38 (T167E) structure (PDB ID: 4BFM) as a search model. The model of MPK38 (T167E) and OTSSP167 were built using Coot [23] and the Refmac program was used for structure refinement [24]. The statistics for data collection and refinement are presented in Table 1. The refined coordinates and structure factor were deposited in the Protein Data Bank (PDB), with the accession number 4CQG.

3. Results and discussion

3.1. Overall structure of MPK38 (T167E) in complex with OTSSP167

The overall structure of the MPK38 (T167E)-OTSSP167 complex is very similar to that of MPK38 (T167E)-AMPPNP, which showing the kinase domain (KD, residues 1–263) and the extended sequence (ExS, residues 264–326), including the UBA linker (residues 264–283) and the UBA domain (residues 284–326) (Fig. 1A). Apart from the disordered activation loop, MPK38 (T167E)-OTSSP167 reflects an active kinase, with αC-in and DFG-in (Fig. 1B). The extensive hydrophobic interactions and hydrogen bond between Arg65 in KD and Thr277/Leu279 in the UBA linker remain in the MPK38 (T167E)-OTSSP167 complex, which function as a clip that maintains the αC helix "in" conformation (Fig. 1C). The electron density map of OTSSP167 is clearly observed in the ATP-binding pocket, as shown in Fig 2A.

3.2. Binding mode of OTSSP167 to MPK38 (T167E)

The molecular structure and atomic numbering of OTSSP167 is shown in Fig. 2B. It has a 1,5-naphthyridine scaffold with trans-4-((dimethylamino)methyl)cyclohexyl)amino group at the 4-position and 3,5-dichloro-4-hydroxyphenyl group at the 6-position. Its inhibitory activity for MELK is 0.41 nM (IC_{50}) [21]. The binding mode of OTSSP167 is shown in Fig. 3.

The 2.57 Å structure of MPK38 (T167E) in complex with OTSSP167 exhibits that its naphthyridine core is stacked between Ile17, Val25, Ala38, and Leu139 and engage in van der Waals interactions with Leu86 (the gatekeeper residue) and Cys70. Additionally, an acetone substituent interacts with the amide carbonyl of Cys89. Except for a hydrogen bond between the N1 atom of naphthyridine core and the main-chain NH of Cys89, the compound does not have any polar interactions with the hinge, but make extensive van der Waals interactions with Glu87 and Tyr88; a short contact (2.9 Å) appears to exist between the C8 of thenaphthyridine core and the main chain carbonyl of Glu87. The cyclohexyl ring of the amide substituent is within van der Waals distance of Val25 and Glu83. The (dimethylamino)methyl group

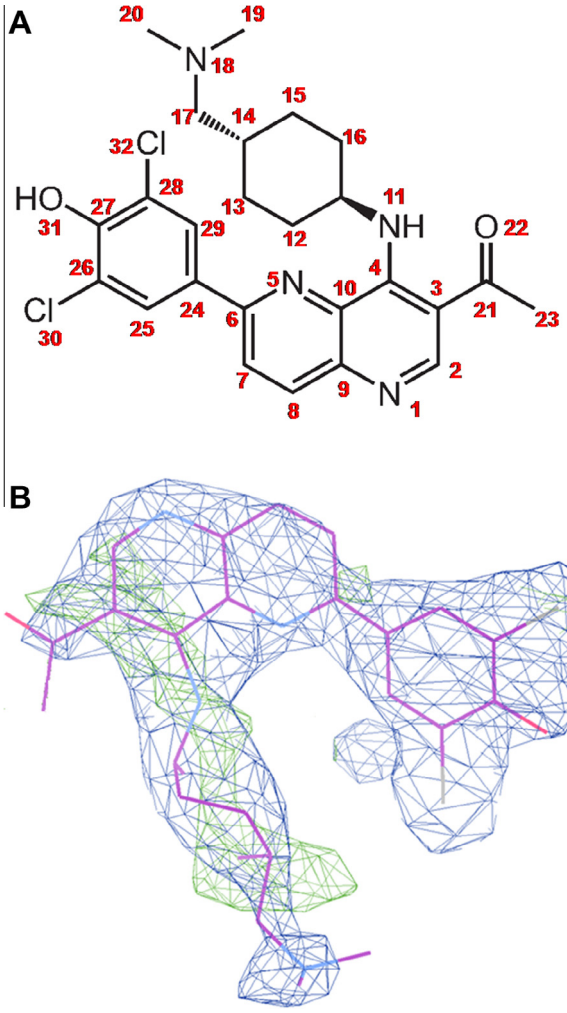

Fig. 2. Chemical structure and the electron density map of OTSSP167. (A) Schematic molecular structure of OTSSP167. (B) The electron density map of OTSSP167 in ATP binding pocket is shown.

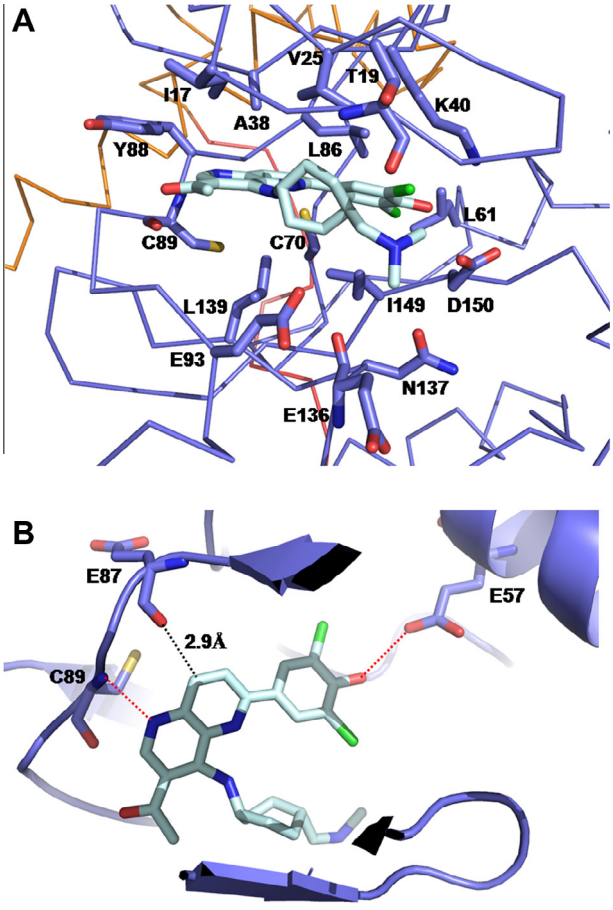

Fig. 3. Binding mode of OTSSP167. (A) Representation of van der Waals interactions between OTSSP167 (cyan) and MPK38 (T167E) active site (blue) is shown. MPK38 (T167E) and its key residues are depicted as C alpha traces and sticks, respectively. (B) Representation of hydrogen bond between OTSSP167 (cyan) and MPK38 (T167E) active site (blue) is shown. The key residues are depicted as sticks and the hydrogen bond is marked as a red dashed line. The short van der Waals contact in the hinge region is also shown as a black dashed line with distance.

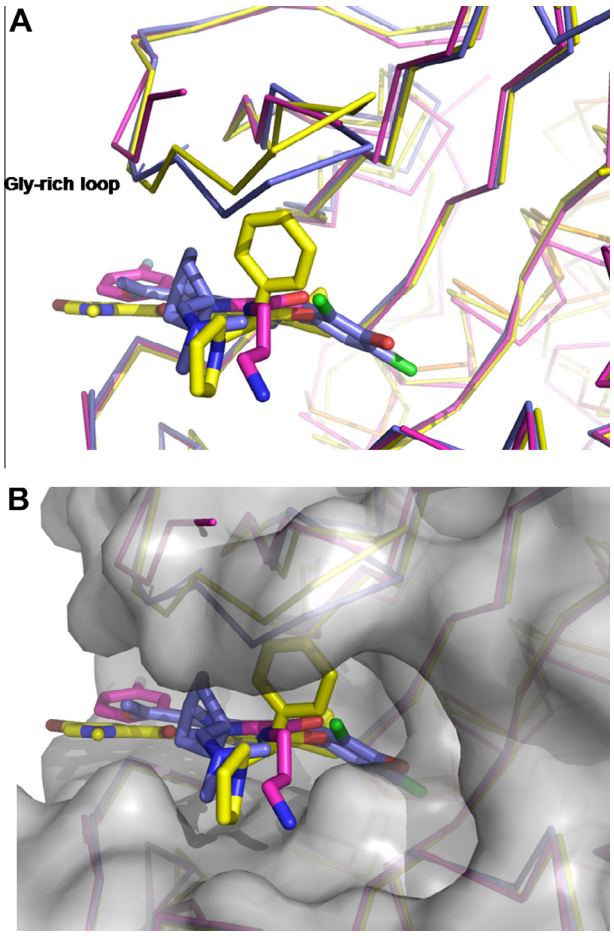

Fig. 4. Superposing of MPK38 (T167E)-OTSSP167 on MELK-Cpd1 and MELK-Cpd2 (A-D) MPK38 (T167E)-OTSSP167 (blue), MELK-Cpd1 (purple), and MELK-Cpd2 (yellow) are shown as C alpha traces and the key residues are depicted as sticks. (A) The glycine-rich loop conformation is shown. (B) The surface of MPK38 (T167E) is displayed in gray color.

undergoes van der Waals interactions with Thr19, Glu136, and Asn137. The phenyl ring of the 3,5-dichloro-4-hydroxyphenyl group at the 6-position is stacked against Leu86 and Ile149. The hydrophobic interactions between its chloride and Leu61 and Leu86 were also observed. Moreover, its hydroxyl group forms a hydrogen bond with the carbonyl group of Glu57 on αC and is within van der Waals distance of Lys40 and Asp150.

3.3. Structural comparison with other MELK-inhibitor complex

At present, the structures of MELK bound to two nanomolar inhibitors, benzodipyrazole Cpd1 (IC_{50} = 27 nM) and pyrrolopyrazole Cpd2 (IC_{50} = 12 nM), are available in PDB [25]. Both compounds present the typical type 1 inhibitor, which is involved in the canonical donor–acceptor hydrogen bonds with the hinge region and bind to the DFG-in conformation [25]. Cpd2 effectively fills the active site by penetrating deeper into the back pocket than Cpd1 and harbors a superior shape complementarity [25].

Fig. 4 shows the superimposition of MPK38 (T167E)-OTSSP167 on MELK-Cpd1 and MELK-Cpd2. The root-mean-square deviation (RMSD) between Cα atoms is 0.55 Å and 0.53 Å, respectively. Although they all display the features of a type 1 inhibitor, several differences were observed. In Cpd1 and Cpd2, it makes the typical donor–acceptor hydrogen bonds with the hinge region [25]. In OTSSP167, it harbors a single hydrogen bond and engaged in very strong van der Waals interactions with the hinge region (Fig 3b). While Cpd1 and Cpd2 are engaged in polar contacts with Glu93, Asn137, and Asp150 via direct or water-mediated hydrogen bonding, OTSSP167 engages in van der Waals interactions with these residues (Fig 3a) [25]. The phenyl group of Cpd2 and the cyclohexyl ring of OTSSP167 stabilize the glycine-rich loop, whereas MELK complexed with Cpd1 exhibits a partially disordered glycine-rich loop (Fig 4a). More importantly, OTSSP167 penetrates ~4 Å deeper into the back pocket than the others and interacts with αC through the dichlorohydroxyphenyl group, perhaps explaining its stronger potency ($IC_{50}$of OTSSP167 = 0.41 nM; Cpd1 = 27 nM; and Cpd2 = 12 nM) (Fig. 4B). The results show that OTSSP167 optimally occupies the active site, especially the hydrophobic back pocket, mainly through van der Waals interactions.

Acknowledgments

We are grateful to the staff scientists at the BL-17A beamline of the Photon Factory and the 5A beamline of the Pohang Light Source for data collection. This work was supported by the Mid-career Researcher Program through a NRF grant funded by the Korea government (MEST) (Nos. 2009-0073145, 2009-0084897, NRF-2012R1A2A2A01012830) and by a grant of the Korea Healthcare Technology R&D project, Ministry for Health, Welfare & Family Affairs, the Republic of Korea (A080320).

References

[1] M. Gil, Y. Yang, Y. Lee, I. Choi, H. Ha, Cloning and expression of a cDNA encoding a novel protein serine/threonine kinase predominantly expressed in hematopoietic cells, Gene 195 (1997) 295–301.
[2] N. Davezac, V. Baldin, J. Blot, B. Ducommun, J.P. Tassan, Human pEg3 kinase associates with and phosphorylates CDC25B phosphatase: a potential role for pEg3 in cell cycle regulation, Oncogene 21 (2002) 7630–7641.
[3] H. Jung, H.A. Seong, H. Ha, Murine protein serine/threonine kinase 38 activates apoptosis signal-regulating kinase 1 via Thr 838 phosphorylation, J. Biol. Chem. 283 (2008) 34541–34553.
[4] M.L. Lin, J.H. Park, T. Nishidate, Y. Nakamura, T. Katagiri, Involvement of maternal embryonic leucine zipper kinase (MELK) in mammary carcinogenesis through interaction with Bcl-G, a pro-apoptotic member of the Bcl-2 family, Breast Cancer Res. 9 (2007) R17.
[5] V. Vulsteke, M. Beullens, A. Boudrez, S. Keppens, A. Van Eynde, M.H. Rider, W. Stalmans, M. Bollen, Inhibition of spliceosome assembly by the cell cycle-regulated protein kinase MELK and involvement of splicing factor NIPP1, J. Biol. Chem. 279 (2004) 8642–8647.
[6] I. Nakano, A.A. Paucar, R. Bajpai, J.D. Dougherty, A. Zewail, T.K. Kelly, K.J. Kim, J. Ou, M. Groszer, T. Imura, W.A. Freije, S.F. Nelson, M.V. Sofroniew, H. Wu, X. Liu, A.V. Terskikh, D.H. Geschwind, H.I. Kornblum, Maternal embryonic leucine zipper kinase (MELK) regulates multipotent neural progenitor proliferation, J. Cell Biol. 170 (2005) 413–427.
[7] D. Gray, A.M. Jubb, D. Hogue, P. Dowd, N. Kljavin, S. Yi, W. Bai, G. Frantz, Z. Zhang, H. Koeppen, F.J. de Sauvage, D.P. Davis, Maternal embryonic leucine zipper kinase/murine protein serine-threonine kinase 38 is a promising therapeutic target for multiple cancers, Cancer Res. 65 (2005) 9751–9761.
[8] I. Nakano, M. Masterman-Smith, K. Saigusa, A.A. Paucar, S. Horvath, L. Shoemaker, M. Watanabe, A. Negro, R. Bajpai, A. Howes, V. Lelievre, J.A. Waschek, J.A. Lazareff, W.A. Freije, L.M. Liau, R.J. Gilbertson, T.F. Cloughesy, D.H. Geschwind, S.F. Nelson, P.S. Mischel, A.V. Terskikh, H.I. Kornblum, Maternal embryonic leucine zipper kinase is a key regulator of the proliferation of malignant brain tumors, including brain tumor stem cells, J. Neurosci. Res. 86 (2008) 48–60.
[9] M.R. Pickard, A.R. Green, I.O. Ellis, C. Caldas, V.L. Hedge, M. Mourtada-Maarabouni, G.T. Williams, Dysregulated expression of Fau and MELK is associated with poor prognosis in breast cancer, Breast Cancer Res. 11 (2009) R60.
[10] J.L. Ku, Y.K. Shin, D.W. Kim, K.H. Kim, J.S. Choi, S.H. Hong, Y.K. Jeon, S.H. Kim, H.S. Kim, J.H. Park, I.J. Kim, J.G. Park, Establishment and characterization of 13 human colorectal carcinoma cell lines: mutations of genes and expressions of drug-sensitivity genes and cancer stem cell markers, Carcinogenesis 31 (2010) 1003–1009.
[11] G. Liu, X. Yuan, Z. Zeng, P. Tunici, H. Ng, I.R. Abdulkadir, L. Lu, D. Irvin, K.L. Black, J.S. Yu, Analysis of gene expression and chemoresistance of CD133+ cancer stem cells in glioblastoma, Mol. Cancer 5 (2006) 67.
[12] B. Ryu, D.S. Kim, A.M. Deluca, R.M. Alani, Comprehensive expression profiling of tumor cell lines identifies molecular signatures of melanoma progression, PLoS One 2 (2007) e594.

[13] S.K. Marie, O.K. Okamoto, M. Uno, A.P. Hasegawa, S.M. Oba-Shinjo, T. Cohen, A.A. Camargo, A. Kosoy, C.G. Carlotti Jr., S. Toledo, C.A. Moreira-Filho, M.A. Zago, A.J. Simpson, O.L. Caballero, Maternal embryonic leucine zipper kinase transcript abundance correlates with malignancy grade in human astrocytomas, Int. J. Cancer 122 (2008) 807–815.
[14] H.D. Hemmati, I. Nakano, J.A. Lazareff, M. Masterman-Smith, D.H. Geschwind, M. Bronner-Fraser, H.I. Kornblum, Cancerous stem cells can arise from pediatric brain tumors, Proc. Natl. Acad. Sci. USA 100 (2003) 15178–15183.
[15] D.R. Rhodes, J. Yu, K. Shanker, N. Deshpande, R. Varambally, D. Ghosh, T. Barrette, A. Pandey, A.M. Chinnaiyan, Large-scale meta-analysis of cancer microarray data identifies common transcriptional profiles of neoplastic transformation and progression, Proc. Natl. Acad. Sci. USA 101 (2004) 9309–9314.
[16] L.W. Hebbard, J. Maurer, A. Miller, J. Lesperance, J. Hassell, R.G. Oshima, A.V. Terskikh, Maternal embryonic leucine zipper kinase is upregulated and required in mammary tumor-initiating cells in vivo, Cancer Res. 70 (2010) 8863–8873.
[17] B.D. Manning, Challenges and opportunities in defining the essential cancer kinome, Sci. Signal 2 (2009) pe15.
[18] J. Brognard, T. Hunter, Protein kinase signaling networks in cancer, Curr Opin Genet Dev 21 (2011) 4–11.
[19] S.W. Cowan-Jacob, H. Mobitz, D. Fabbro, Structural biology contributions to tyrosine kinase drug discovery, Curr. Opin. Cell Biol. 21 (2009) 280–287.
[20] J. Zhang, P.L. Yang, N.S. Gray, Targeting cancer with small molecule kinase inhibitors, Nat. Rev. Cancer 9 (2009) 28–39.
[21] S. Chung, H. Suzuki, T. Miyamoto, N. Takamatsu, A. Tatsuguchi, K. Ueda, K. Kijima, Y. Nakamura, Y. Matsuo, Development of an orally-administrative MELK-targeting inhibitor that suppresses the growth of various types of human cancer, Oncotarget 3 (2012) 1629–1640.
[22] A.A. Vagin, M.N. Isupov, Spherically averaged phased translation function and its application to the search for molecules and fragments in electron-density maps, Acta. Crystallogr. D Biol. Crystallogr. 57 (2001) 1451–1456.
[23] P. Emsley, B. Lohkamp, W.G. Scott, K. Cowtan, Features and development of Coot, Acta Crystallogr D BiolCrystallogr 66 (2010) 486–501.
[24] P.D. Adams, P.V. Afonine, G. Bunkoczi, V.B. Chen, I.W. Davis, N. Echols, J.J. Headd, L.W. Hung, G.J. Kapral, R.W. Grosse-Kunstleve, A.J. McCoy, N.W. Moriarty, R. Oeffner, R.J. Read, D.C. Richardson, J.S. Richardson, T.C. Terwilliger, P.H. Zwart, PHENIX: a comprehensive Python-based system for macromolecular structure solution, Acta Crystallogr D BiolCrystallogr 66 (2010) 213–221.
[25] G. Canevari, S. Re, Depaolini, U. Cucchi, J.A. Bertrand, E. Casale, C. Perrera, B. Forte, P. Carpinelli, E.R. Felder, Structural insight into maternal embryonic leucine zipper kinase (MELK) conformation and inhibition toward structure-based drug design, Biochemistry 52 (2013) 6380–6387.